



Cite this: *Chem. Commun.*, 2024, **60**, 5534

Received 31st January 2024,
Accepted 23rd April 2024

DOI: 10.1039/d4cc00488d

rsc.li/chemcomm

We present a gram-scale synthesis of metallocdielectric Janus matchsticks, which feature a gold-coated silica sphere and a silica rod. SiO_2 Janus matchsticks are synthesized in one batch by growing amine-functionalized SiO_2 spheres at the end of SiO_2 rods. Gold deposition on the spheres produces $\text{Au}-\text{SiO}_2$ Janus matchsticks with an aspect ratio controlled by the rod length. The metallocdielectric Janus matchsticks, produced by scalable colloidal synthesis, hold great potential as functional colloidal materials.

Janus particles feature an asymmetric structure with two distinct physical and/or chemical characteristics.^{1–3} They have been studied in a wide range of fundamental investigations including stabilization of multiphasic mixture,^{4–6} micromotors and active colloids,^{7–9} and colloidal self-assembly.^{10–12} Metallocdielectric Janus particles are a particular type of anisotropic colloids that comprise metallic and dielectric regions. They have been studied as active colloids that exhibit dynamic propulsion and assembly activated by chemical or external field.¹³ For instance, platinum-coated Janus spheres are able to self-propel by decomposing a fuel such as hydrogen peroxide.^{14,15} Gold-coated Janus and patchy colloids have been demonstrated with a variety of propulsion and assembly behaviors when activated by an AC electric field.^{16–18}

A straightforward way of making these particles is by physical vapor deposition (PVD), whereby a thin metal film is coated on a monolayer of dielectric spheres while enabling the shape of the metal patch *via* glancing angle deposition.^{19,20} The method, however, is limited by scalability and does not provide much control over the particle geometry. Recent developments

in colloidal synthesis have provided metallocdielectric Janus particles with more sophisticated shape control.^{21,22} For instance, the platinum-polystyrene Janus dimers have been synthesized by a sequential chemical deposition of gold and platinum onto the lobe with amine groups.²³ Recently, a “cluster-encapsulation-dewetting” method has been developed for making Janus particles (two lobes) and patchy particles (multiple lobes).^{24–26} The aspect ratio of Janus particles can be controlled by the dewetting degree of the two lobes. After coating gold on the lobes, these particles can be stimulated to propel or rotate, and form spinning clusters or colloidal molecules under AC electric field.²⁷ However, the current synthetic methods involve multiple steps and are not suitable for mass production of metallocdielectric Janus particles. Therefore, while these particles offer a great model system for exploring the dynamic behaviors of active colloids, their material functions have been largely overlooked due to the lack of facile and scalable synthetic methods.

Herein, we develop a gram-scale colloidal synthesis of gold-silica Janus matchsticks with a tunable aspect ratio. These Janus matchsticks are made of a gold-coated silica sphere and a straight silica rod. SiO_2 Janus matchsticks are synthesized by sequentially adding a silane ((3-aminopropyl)triethoxysilane, APTES) and the silica precursor (tetraethyl orthosilicate, TEOS) to the as-synthesized SiO_2 rod suspension. The APTES hydrolyzes and remains soluble in the water droplet attached to the SiO_2 rod, which not only increases the droplet's volume and transforms the rod to the matchstick shape, but also modifies it with amine groups. The condensation of TEOS with APTES solidifies the water droplet and fixes the matchstick shape. A gold nanolayer is selectively coated on the amine-functionalized SiO_2 sphere, resulting in the $\text{Au}-\text{SiO}_2$ Janus matchsticks. Our work will enable future studies on their active propulsions and potential applications in optical devices.

The synthesis of metallocdielectric Janus matchsticks is schematically illustrated in Fig. 1. A key step for creating the matchstick shape is to modify the silica growth in the water droplet from the rod by sequentially adding (3-aminopropyl)triethoxysilane (APTES) followed by tetraethyl orthosilicate (TEOS). Given the different

^a Department of Chemical and Biomolecular Engineering, University of Pennsylvania, Philadelphia, Pennsylvania, 19104, USA.
E-mail: daeyeon@seas.upenn.edu

^b Department of Chemistry, The University of Hong Kong, Pokfulam Road, Hong Kong, China

^c Department of Chemistry and Chemical Biology, Northeastern University, Boston, MA 02115, USA

† Electronic supplementary information (ESI) available. See DOI: <https://doi.org/10.1039/d4cc00488d>



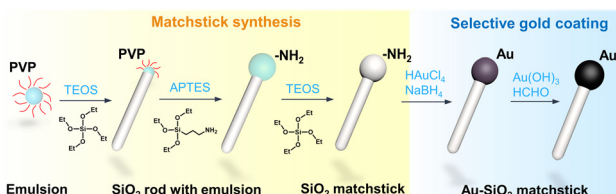


Fig. 1 Schematic showing the synthesis of SiO_2 matchstick with an amine-functionalized head and the site-specific gold coating to form $\text{Au}-\text{SiO}_2$ matchstick.

chemical structures, APTES and its hydrolyzed products are soluble in the water droplet which expands its size; this process transforms the rod into the matchstick shape. If TEOS is added first, however, its hydrolysis in the water droplet would simply extend the rod length. The introduction of different silanes, such as hexadecyltrimethoxysilane, to the rod suspension has also been used to make amphiphilic Janus particles.^{28,29} In this case, the silane and TEOS are added as a mixture, by which the rods become partially functionalized by the silane.

A detailed description of the synthesis is as follows: first, SiO_2 rods are synthesized following a previous method.³⁰ Water-in-oil (W/O) emulsions are generated in a solution mixture containing water, pentanol, polyvinylpyrrolidone (PVP), ammonia, and sodium citrate. The addition and hydrolysis of the silica precursor, TEOS, forms solid SiO_2 in the water droplets. The water droplet partially engulfs the solid SiO_2 rather than fully wetting it; thus, the subsequent silica growth occurs at the interface of this solid SiO_2 and the droplet and occurs along one dimension, producing a straight SiO_2 rod.

After the growth of SiO_2 rod, a silane, APTES, is added to the rod suspension of same batch. APTES hydrolysis in the water droplet forms soluble oligomers, which do not induce further growth of the rod but rather introduce amine groups in the droplet. At the same time, the size of the water droplet increases with the addition of APTES, converting the SiO_2 rod into a matchstick particle. To solidify the water droplet and fix the matchstick shape, TEOS is added again and its condensation with APTES oligomers forms the crosslinked SiO_2 sphere (*i.e.*, the head of the matchstick).

Water droplets attached at the rod end can be observed under an optical microscope in some SiO_2 rods with large diameters (Fig. 2a). After the subsequent addition of APTES and TEOS, the SiO_2 Janus matchsticks are obtained, as shown in Fig. 2b. To verify that only the spherical heads are functionalized with amine groups, we use a fluorescent dye, fluorescein isothiocyanate (FITC-NCS), where the NCS group forms a covalent bond with the NH_2 group. Confocal microscopy of these particles clearly shows that the fluorescence signal is only detected on the spherical head of the matchstick as shown in Fig. 2c.

The SiO_2 sphere with amine groups is selectively coated with a gold nanolayer, yielding the $\text{Au}-\text{SiO}_2$ Janus matchsticks. The gold coating is performed by a two-step seeding and growth protocol.²⁴ Specifically, the amine groups can chemically bind a gold precursor (chloroauric acid, HAuCl_4),³¹ which is reduced to gold nanoparticles on the surface of the silica sphere. The

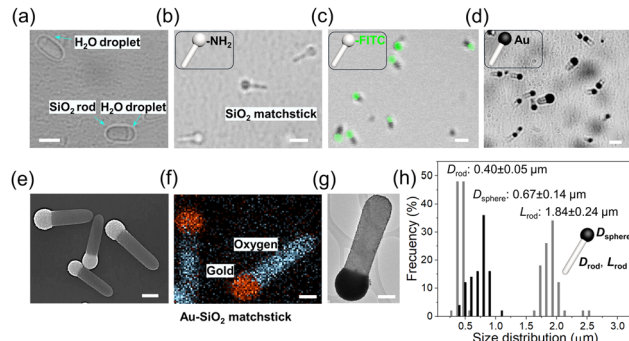


Fig. 2 (a) Optical microscope image showing water droplets attached at the end of SiO_2 rods. (b) Optical microscope image of the SiO_2 Janus matchsticks. (c) Confocal microscope image showing that the fluorescent dye, fluorescein isothiocyanate (FITC-NCS) is selectively grafted to the spherical heads of matchstick particles. (d) Optical microscope image of the $\text{Au}-\text{SiO}_2$ Janus matchsticks. Scale bars = 1 μm . (e) Scanning electron microscope (SEM) image of the $\text{Au}-\text{SiO}_2$ Janus matchsticks. (f) Energy dispersive X-ray (EDX) image of gold and oxygen. Scale bars = 0.5 μm . (g) Transmission electron microscope (TEM) image of the $\text{Au}-\text{SiO}_2$ Janus matchstick, scale bar = 200 nm. (h) Distribution of length of rod, diameter of rod and sphere based on counting at least 50 $\text{Au}-\text{SiO}_2$ Janus matchsticks.

gold nanoparticles serve as seeds for the further growth of the gold nanolayer covering the spherical SiO_2 head (Fig. 2d). The change in the appearance of Janus matchsticks during the gold coating process is shown in Fig. S1 (ESI[†]).

The gold nanolayers remain attached to the silica spheres after sonication and several rounds of centrifugation-redispersion process. We believe that the robust adhesion observed can be attributed to the chemical adsorption of gold seeds onto amine-functionalized spheres, as opposed to physical adsorption. Furthermore, the subsequent gold growth step further reinforces the attachment to the silica sphere. If only the first step of gold coating is conducted, the spherical heads of Janus matchsticks appear grey under optical microscope (Fig. S1b, ESI[†]), suggesting that the amount of gold coating is limited.

Scanning electron microscopy (SEM) and energy dispersive X-ray (EDX) images of these particles clearly demonstrate the formation of gold layers on the spherical heads of matchstick particles as shown in Fig. 2e and f. In addition, transmission electron microscope (TEM) images of $\text{Au}-\text{SiO}_2$ Janus matchsticks are shown in Fig. 2g and Fig. S3b (ESI[†]). While it is difficult to distinguish the gold film from the spherical head, gold nanoparticles with the diameter of ~ 4 nm are observed at the edge of the sphere and more than a single layer of such gold nanoparticles are present. The average rod length is $1.84 \pm 0.24 \mu\text{m}$ and the average diameter of rod and sphere is 0.40 ± 0.05 and $0.67 \pm 0.14 \mu\text{m}$, respectively, as shown in Fig. 2h.

We note that the addition of TEOS must follow the complete hydrolysis of APTES within water droplets, which normally takes a few hours (*e.g.*, 5 h). If TEOS and APTES are added simultaneously as a mixture to the as-synthesized rod suspension, their condensation induces the growth of a tail-like silica tip at the rod end instead of a spherical head, as shown in Fig. 3a–c. Under these conditions, the rods from the particles can be coated with gold, suggesting that the amine functionalization is not



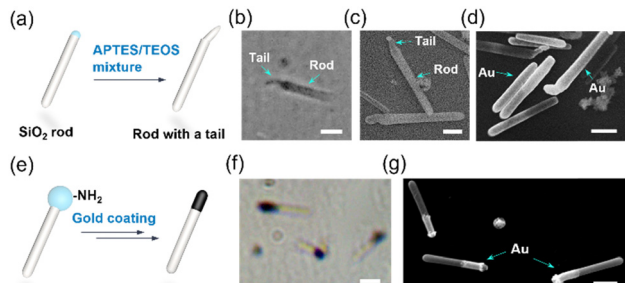


Fig. 3 (a)–(c) Schematic, optical microscope and SEM images showing that adding APTES and TEOS as a mixture forms a silica tail at the end of rod. (d) SEM image shows that rods are coated with gold. (e) Schematic illustration showing gold coating on matchsticks in the absence of TEOS addition. (f)–(g) Optical microscope and SEM images show that gold is selectively coated at the tip of the rods where water droplets were attached. Scale bars = 1 μ m.

site-specific (Fig. 3d). Our data suggests that the sequential addition of APTES and TEOS is essential for making the Au–SiO₂ Janus matchsticks. If TEOS is not added after APTES, then the water droplet containing hydrolyzed APTES dissolves in water, which results in the removal of the spherical head. We find that one tip of these rods is selectively coated with gold (Fig. 3e–g). This may be due to functionalization of the silica rod ends with amine groups prior to the dissolution of water droplets.

In addition, the concentration of APTES or the ratio of APTES and TEOS can also influence the morphology of the Janus matchsticks. As shown in Fig. S4 (ESI[†]), when the concentration of APTES is lower than 21 mM at the constant concentration of TEOS (45 mM), some of the SiO₂ rods on the matchsticks are longer and become curly; and in some matchsticks, there are tails that grow from the spherical heads. For all these experiments, gold is found to be only coated on the spherical heads of matchsticks.

We further demonstrate that the aspect ratio of the gold and silica in the Janus matchsticks can be tuned by changing the length of SiO₂ rods. Specifically, the diameter of gold-coated sphere is generally fixed at around 0.7 μ m as it is determined by the diameter of the SiO₂ rod (around 0.4 μ m) shown in Fig. 2g. The length of SiO₂ rod can be synthetically tuned from 0.8 μ m to 2 μ m by the volume of TEOS for the rod growth, as shown in Fig. 4a. The colloidal synthesis protocol allows scale-up of the reaction volume of SiO₂ Janus matchsticks from 5 mL to 100 mL; subsequent gold coating following the same procedure as described above yields Au–SiO₂ matchstick particles in >1 gram quantity (Fig. 4b and c). Such scalability is critical for practical applications of these metallocodielectric Janus matchsticks with shape and chemical anisotropy.

In summary, we have demonstrated a scalable colloidal synthesis of Au–SiO₂ Janus matchsticks consisting of a gold-coated sphere and a silica rod. We find that the sequential addition of APTES and TEOS to the SiO₂ rod suspension leads to growth of an amine functionalized sphere at the end of SiO₂ rod, therefore forming the matchstick geometry. Taking advantage of the anisotropic surface chemistry, gold is selectively

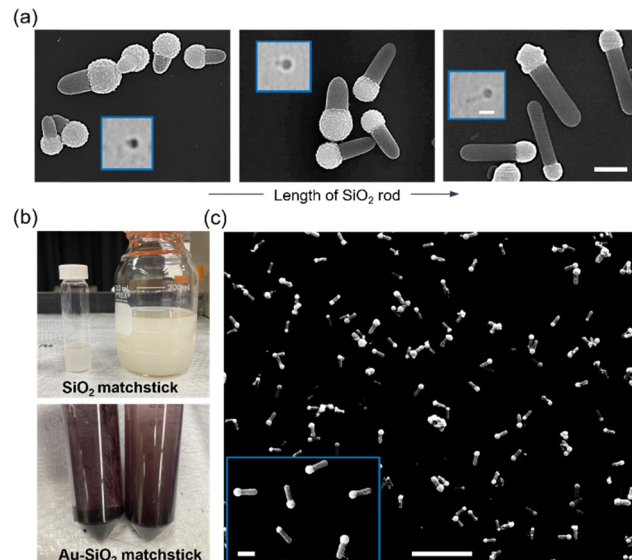


Fig. 4 (a) SEM images of the Au–SiO₂ Janus matchsticks with a tunable aspect ratio. Insets are the corresponding microscope images of SiO₂ Janus matchsticks before gold coating. Scale bars = 1 μ m. (b) Pictures showing the ability to increase the reaction volume and produce Au–SiO₂ Janus matchsticks in gram scale. (c) A zoom-out SEM image of Au–SiO₂ Janus matchsticks. Scale bar = 10 μ m. Inset is the zoom-in image. Scale bar = 1 μ m.

coated on the spherical head of the matchstick. Both steps are scalable enabling gram-scale production of Au–SiO₂ Janus matchsticks. Our future studies will focus on investigating the optical and plasmonic properties of these metallocodielectric Janus matchsticks. Moreover, the motion of these gold-coated particles can be driven by AC electric field by the effects of induced-charge electrophoresis (ICEP), electrohydrodynamic (EHD) flow, self-dielectrophoresis (sDEP), which would be a rich area for future investigations.

Y. M. and W. D. conceived the project. Y. M. and D. L. wrote the manuscript. W. D., Y. D., P. S., L. D. and Y. W. participated in the manuscript revision. All authors have given approval to the final version of the manuscript.

We would like to acknowledge the support of DARPA (FA8650-22-C-7208). Approved for Public Release, Distribution Unlimited. The views, opinions and/or findings expressed are those of the author and should not be interpreted as representing the official views or policies of the Department of Defense or the U.S. Government. We would like to thank Dr. Douglas M. Yates, Director of Nanoscale Characterization Facility at University of Pennsylvania, for helping with the TEM characterization.

Conflicts of interest

There are no conflicts to declare.

Notes and references

- J. Hu, S. Zhou, Y. Sun, X. Fang and L. Wu, *Chem. Soc. Rev.*, 2012, **41**, 4356–4378.
- J. Zhang, B. A. Grzybowski and S. Granick, *Langmuir*, 2017, **33**, 6964–6977.



3 L. C. Bradley, W.-H. Chen, K. J. Stebe and D. Lee, *Curr. Opin. Colloid Interface Sci.*, 2017, **30**, 25–33.

4 F. Tu and D. Lee, *J. Am. Chem. Soc.*, 2014, **136**, 9999–10006.

5 L. C. Bradley, K. J. Stebe and D. Lee, *J. Am. Chem. Soc.*, 2016, **138**, 11437–11440.

6 B. J. Park and D. Lee, *ACS Nano*, 2012, **6**, 782–790.

7 A. Aubret, M. Youssef, S. Sacanna and J. Palacci, *Nat. Phys.*, 2018, **14**, 1114–1118.

8 Y. Mu, W. Duan, K. Y. Hsu, Z. Wang, W. Xu and Y. Wang, *ACS Appl. Mater. Interfaces*, 2022, **14**, 57113–57121.

9 W. F. Paxton, K. C. Kistler, C. C. Olmeda, A. Sen, S. K. St. Angelo, Y. Cao, T. E. Mallouk, P. E. Lammert and V. H. Crespi, *J. Am. Chem. Soc.*, 2004, **126**, 13424–13431.

10 Q. Chen, J. K. Whitmer, S. Jiang, S. C. Bae, E. Luijten and S. Granick, *Science*, 2011, **331**, 199–202.

11 J. S. Oh, S. Lee, S. C. Glotzer, G. R. Yi and D. J. Pine, *Nat. Commun.*, 2019, **10**, 3936.

12 T. Zhang, D. Lyu, W. Xu, X. Feng, R. Ni and Y. Wang, *Nat. Commun.*, 2023, **14**, 8494.

13 N. M. Diwakar, G. Kunti, T. Miloh, G. Yossifon and O. D. Velev, *Curr. Opin. Colloid Interface Sci.*, 2022, **59**, 101586.

14 J. Zhang, X. Zheng, H. Cui and Z. Silber-Li, *Micromachines*, 2017, **8**, 123.

15 X. Lyu, X. Liu, C. Zhou, S. Duan, P. Xu, J. Dai, X. Chen, Y. Peng, D. Cui, J. Tang, X. Ma and W. Wang, *J. Am. Chem. Soc.*, 2021, **143**, 12154–12164.

16 J. Yan, M. Han, J. Zhang, C. Xu, E. Luijten and S. Granick, *Nat. Mater.*, 2016, **15**, 1095–1099.

17 J. Zhang, J. Yan and S. Granick, *Angew. Chem., Int. Ed.*, 2016, **55**, 5166–5169.

18 Z. Wang, Z. Wang, J. Li and Y. Wang, *ACS Nano*, 2021, **15**, 5439–5448.

19 J. G. Lee, A. M. Brooks, W. A. Shelton, K. J. M. Bishop and B. Bharti, *Nat. Commun.*, 2019, **10**, 2575.

20 Q. Chen, S. C. Bae and S. Granick, *Nature*, 2011, **469**, 381–384.

21 T. Hueckel, G. M. Hocky and S. Sacanna, *Nat. Rev. Mater.*, 2021, **6**, 1053–1069.

22 Z. Wang, Y. Mu, D. Lyu, M. Wu, J. Li, Z. Wang and Y. Wang, *Curr. Opin. Colloid Interface Sci.*, 2022, **61**, 101608.

23 S. Wang and N. Wu, *Langmuir*, 2014, **30**, 3477–3486.

24 Z. Wang, Z. Wang, J. Li, S. T. H. Cheung, C. Tian, S. H. Kim, G. R. Yi, E. Ducrot and Y. Wang, *J. Am. Chem. Soc.*, 2019, **141**, 14853–14863.

25 X. Zheng, M. Liu, M. He, D. J. Pine and M. Weck, *Angew. Chem., Int. Ed.*, 2017, **56**, 5507–5511.

26 F. Dong, S. Munkaila, V. Grebe, M. Weck and M. D. Ward, *Soft Matter*, 2022, **18**, 7975–7980.

27 Z. Wang, Z. Wang, J. Li, C. Tian and Y. Wang, *Nat. Commun.*, 2020, **11**, 2670.

28 J. He, M. J. Hourwitz, Y. Liu, M. T. Perez and Z. Nie, *Chem. Commun.*, 2011, **47**, 12450–12452.

29 J. He, B. Yu, M. J. Hourwitz, Y. Liu, M. T. Perez, J. Yang and Z. Nie, *Angew. Chem., Int. Ed.*, 2012, **51**, 3628–3633.

30 A. Kuijk, A. van Blaaderen and A. Imhof, *J. Am. Chem. Soc.*, 2011, **133**, 2346–2349.

31 J. S. Oh, L. N. Dang, S. W. Yoon, P. C. Lee, D. O. Kim, K. J. Kim and J. D. Nam, *Macromol. Rapid Commun.*, 2013, **34**, 504–510.

